ISSN 1674-1056
http://cpb.iphy.ac.cn
http://iopscience.iop.org/cpb
中国物理 B
Chinese Physics
中国物理
Chinese Physics B

Low temperature photoluminescence study of GaAs defect states

Jia-Yao Huang(黄佳瑶)[1], Lin Shang(尚林)[1], Shu-Fang Ma(马淑芳)[1], Bin Han(韩斌)[1], Guo-Dong Wei(尉国栋)[1], Qing-Ming Liu(刘青明)[1], Xiao-Dong Hao(郝晓东)[1], Heng-Sheng Shan(单恒升)[1], Bing-She Xu(许并社)[1,2]

Citation: Chin. Phys. B . 2020, 29(1): 010703 . **doi:** 10.1088/1674-1056/ab5fb8
Journal homepage: http://cpb.iphy.ac.cn; http://iopscience.iop.org/cpb

What follows is a list of articles you may be interested in

Development of a 170-mm hollow corner cube retroreflector for the future lunar laser ranging

Yun He(何芸), Qi Liu(刘祺), Jing-Jing He(何静静), Ming Li(黎明), Hui-Zong Duan(段会宗), Hsien-Chi Yeh(叶贤基), Jun Luo(罗俊)

Chin. Phys. B . 2018, 27(10): 100701 . **doi:** 10.1088/1674-1056/27/10/100701

Co-focus experiment of segmented mirror

Bin Li(李斌), Wen-Hao Yu(于文豪), Mo Chen(陈莫), Jin-Long Tang(唐金龙), Hao Xian(鲜浩)

Chin. Phys. B . 2017, 26(6): 060706 . **doi:** 10.1088/1674-1056/26/6/060706

STED microscopy based on axially symmetric polarized vortex beams

Zhehai Zhou(周哲海), Lianqing Zhu(祝连庆)

Chin. Phys. B . 2016, 25(3): 030701 . **doi:** 10.1088/1674-1056/25/3/030701

Piecewise spectrally band-pass for compressive coded aperture spectral imaging

Qian Lu-Lu, Lü Qun-Bo, Huang Min, Xiang Li-Bin

Chin. Phys. B . 2015, 24(8): 080703 . **doi:** 10.1088/1674-1056/24/8/080703

Design and fabrication of structural color by local surface plasmonic meta-molecules

Ma Ya-Qi, Shao Jin-Hai, Zhang Ya-Feng, Lu Bing-Rui, Zhang Si-Chao, Sun Yan, Qu Xin-Ping, Chen Yi-Fang

Chin. Phys. B . 2015, 24(8): 080702 . **doi:** 10.1088/1674-1056/24/8/080702

Low temperature photoluminescence study of GaAs defect states*

Jia-Yao Huang(黄佳瑶)[1], Lin Shang(尚林)[1], Shu-Fang Ma(马淑芳)[1,‡], Bin Han(韩斌)[1], Guo-Dong Wei(尉国栋)[1], Qing-Ming Liu(刘青明)[1], Xiao-Dong Hao(郝晓东)[1], Heng-Sheng Shan(单恒升)[1], and Bing-She Xu(许并社)[1,2,†]

[1] *Institute of Atomic and Molecular Science, Shaanxi University of Science and Technology, Xi'an* 710021, *China*
[2] *Key Laboratory of Interface Science and Engineering in Advanced Materials of Ministry of Education, Taiyuan University of Technology, Taiyuan* 030024, *China*

(Received 26 August 2019; revised manuscript received 17 November 2019; accepted manuscript online 9 December 2019)

Low temperature (77 K) photoluminescence measurements have been performed on different GaAs substrates to evaluate the GaAs crystal quality. Several defect-related luminescence peaks have been observed, including 1.452 eV, 1.476 eV, 1.326 eV peaks deriving from 78 meV Ga_{As} antisite defects, and 1.372 eV, 1.289 eV peaks resulting from As vacancy related defects. Changes in photoluminescence emission intensity and emission energy as a function of temperature and excitation power lead to the identification of the defect states. The luminescence mechanisms of the defect states were studied by photoluminescence spectroscopy and the growth quality of GaAs crystal was evaluated.

Keywords: low temperature photoluminescence, Ga_{As} antisite defects, luminescence mechanisms of defect states, GaAs crystal quality

PACS: 07.60.–j, 81.05.–t, 81.05.Ea **DOI:** 10.1088/1674-1056/ab5fb8

1. Introduction

The growth quality of GaAs substrate and its epilayer is very important for device performance such as laser diodes (LDs),[1] heterojunction bipolar transistors (HBTs), and high electron mobility transistors (HEMTs).[2] For this reason, the identification and characterization of defects in GaAs substrate, as well as the understanding of their optical and thermodynamical properties, are very important and remain an active research field.[3–7] There are six elementary native point defect species in GaAs substrate: vacancies in the Ga sublattice (V_{Ga}), vacancies in the As sublattice (V_{As}), Ga self-interstitials (I_{Ga}), As self-interstitials (I_{As}), antisite defects formed by a Ga atom on an As site (Ga_{As}) and an As atom on a Ga site (As_{Ga}).[8] V_{As} and Ga_{As} are at $E_C - 0.145$ eV and $E_V + 0.078$ eV, respectively.[9] The spectral features of these defects in the photoluminescence (PL) spectra of GaAs have been studied.[3,10–13]

PL is very sensitive to lattice perfection and has been extensively used to characterize the impurity and defect energy levels in GaAs.[14–17] The characterization of GaAs substrates is of great significance for improving the crystal growth quality of the epitaxial layers. The defects and their luminescence mechanisms can be identified by measuring the temperature and excitation power dependence of the GaAs PL. However, very little information regarding excitation power and temperature dependence of the GaAs PL have appeared in the literature.

In this article, a scientifically investigation on the PL measurement of different samples is performed. The purpose of this paper is to study the luminescence mechanism of defects and determine the GaAs crystal quality. The dependences of the peak positions, intensities, and shapes of the PL spectra on temperature and laser excitation power were investigated. Different PL peaks at 1.476 eV, 1.452 eV, 1.372 eV, 1.326 eV, and 1.289 eV appeared and optical transition models were established to analyze the defect states and their luminescence mechanisms.

2. Experimental details

In this study, (100)-oriented, 2-inches, Te/Si-doped GaAs samples grown by the liquid-encapsulated Czochralski (LEC) method were obtained from a commercial vendor. Three samples with different carrier concentrations ranging from 10^{15} cm^{-3} to 10^{18} cm^{-3} were investigated. The thickness of all three GaAs substrates was 350 μm. The description of the GaAs samples is given in Table 1.

The samples were mounted on a vacuum copper platform. The PL spectra of the GaAs samples were detected in an optical cryostat at temperature from 77 K to 300 K in a liquid nitrogen atmosphere. For PL excitation, we used the focused radiation of a 532 nm laser with photon energy of 2.33 eV and the power reached 150 mW. The spectral resolution in all cases was better than 0.1 nm. The PL signals were collected by the HORIBA MicOS-iHR320 series variable temperature micro-PL spectrometer.

*Project supported by the National Natural Science Foundation of China (Grant No. 21972103), the National Key Research and Development Program of China (Grant No. 2016YFB040183), and Research and Development Program of Shanxi Province, China (Grant No. 201703D111026).

†Corresponding author. E-mail: xubs@tyut.edu.cn
‡Corresponding author. E-mail: mashufang@sust.edu.cn

© 2020 Chinese Physical Society and IOP Publishing Ltd

Table 1. Description of GaAs samples used in this work.

Sample	Dopant	Carrier concentration/cm^{-3}	Dislocation density/cm^{-2}	Doping type
M1	Te	$\sim 10^{16}$	< 500	N
M2	Si	$\sim 10^{15}$	500	N
M3	Si	$\sim 10^{18}$	5000	N

3. Results and discussion

Figure 1 shows the PL spectra of the GaAs samples at 77 K. Figure 1(a) shows the PL spectra of the Te-doped GaAs sample at 77 K. The emission peak at 821 nm is due to the band-to-band transition of GaAs.[8] The emission peak at 979 nm is attributed to the Te_{As}–V_{Ga} transition.[16,18] Moreover, in Fig. 1(a), it is worth noting that the full widths at half maximum (FWHMs) of the 821 nm and 979 nm peaks are 13 nm and 62 nm, respectively, which also show the high peak intensity ratio. In Fig. 1(b), the emission peak at 823 nm is due to the band-to-band transition of GaAs. The emission peaks of 854 nm and 935 nm originate from the free electron to neutral acceptor transition (e, A^0) and the free electron to the ionized acceptor (e, A^-) transition, respectively.[19] The luminescence behavior associated with such localized centers has been successfully explained by the isolated gallium antisite (Ga_{As}), 78 meV/203 meV double-acceptor defect in GaAs.[12,13,20–23] In Fig. 1(c), there are three classes of emission peaks observed in the PL spectra. The intrinsic luminescence peak of GaAs at 77 K disappears, and the remained emission peaks at 840 nm and 904 nm are due to Ga_{As},[24] V_{As} to Si_{As} transitions,[8] respectively. The 962 nm emission peak is attributed to the V_{As} to Ga_{As} complex transition. The origin of these peaks is discussed in detail below. It can be observed that the intensity of band-to-band transition in sample M1 is dominated. As a consequence, we conclude that the growth quality of sample M1 is the best.

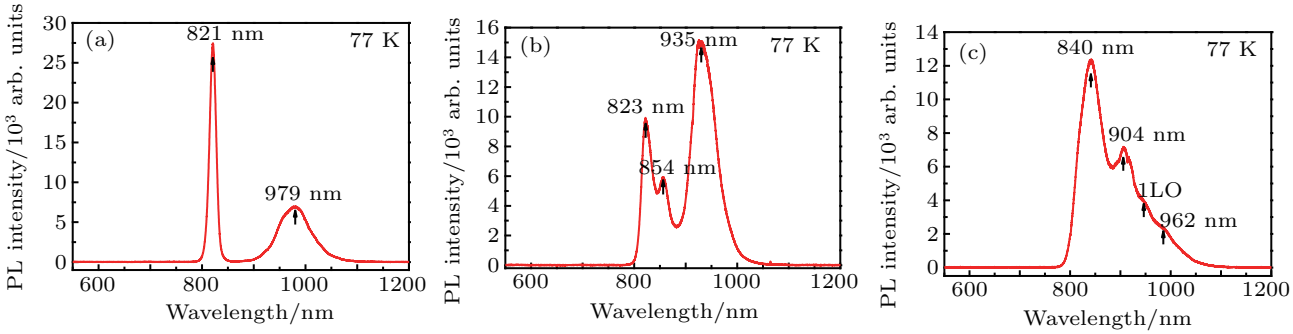


Fig. 1. Photoluminescence spectra of the Te and Si-doped GaAs samples at 77 K: (a) sample M1, Te-doped GaAs crystal, (b) sample M2, Si-doped GaAs crystal, (c) sample M3, Si-doped GaAs crystal.

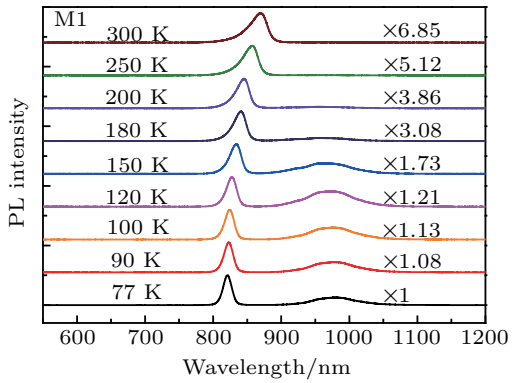


Fig. 2. The normalized PL spectra taken at various temperatures of sample M1, the Te-doped GaAs sample.

Figure 2 displays the typical PL spectra of the Te-doped GaAs crystals taken at various temperatures. For the intrinsic peak emission in the GaAs PL spectra, the relationship between the peak-energy position and temperature can be described by

$$E_g = 1.519 - 5.405 \times 10^{-4} \times \frac{T^2}{(T + 204)} \quad (\text{eV}), \qquad (1)$$

where E_g is the band-gap energy, and T is the measurement temperature. In this case, the emission peak of sample M1 locates at 821 nm (1.510 eV) at 77 K, which is consistent with Eq. (1). It can be observed that the intensity of the band-to-band transition is dominated as the temperature increases from 77 K to 300 K. This implies that the growth quality of sample M1 is good. Up to 150 K, the PL spectra of sample M1 show a peak of Te_{As}–V_{Ga} transition. As the temperature increases, the lattice vibrations become intense, and the interaction between electrons and phonons is also enhanced, resulting in the nonradiative recombination predominating, leading to the quenching of the defect state Te_{As}–V_{Ga} transition.

Figure 3(a) shows the temperature-dependence PL spectra of the Si-doped GaAs sample. Such material also possesses an acceptor level at 78 meV above the valence band. It has been confirmed that the center is a double acceptor, Ga_{As}, with the first and second ionization energies of 78 meV and 200 meV, respectively.[20,25] The authors discovered that GaAs grown by the LEC technique from Ga rich melts developed Ga_{As} antisite defects and As vacancy. In the low-temperature PL measurements, peak B occurring at 854 nm (1.452 eV) presumably corresponds to an electron transition to the neutral acceptor (e, A^0) associated with the 78 meV level Ga_{As}.[12,13,26] Peak C centered at about 935 nm (1.326 eV) corresponds to

200 meV above valence band Ga_{As}^{2-} antisite defect, involving the free electron to ionized acceptor transition (e, A^-). For the (e, A^0) transition, the defect center must trap two photoexcited holes, while the (e, A^-) transition requires trapping of only one photoexcited hole by the center.

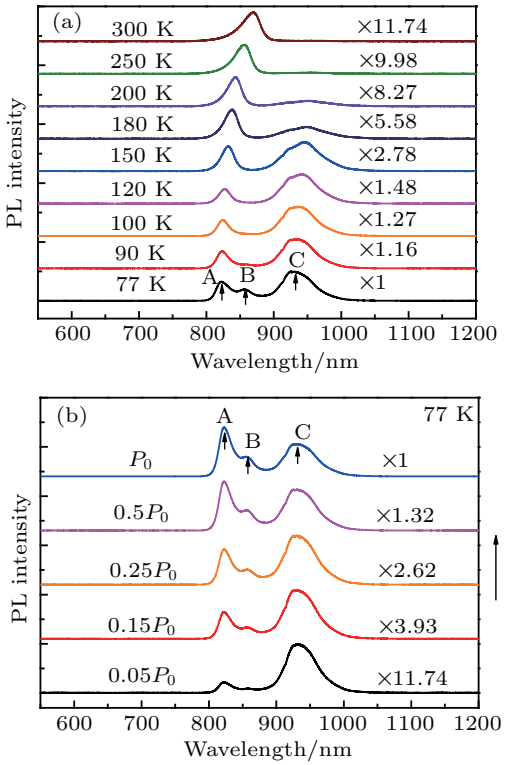


Fig. 3. PL spectra of sample M2, the Si-doped GaAs crystal. (a) The normalized PL spectra taken at various temperatures. (b) The normalized PL spectra taken at various excitation power at 77 K. The direction of the arrow represents an increase in the excitation power.

The emission intensities of peaks B and C decrease quite rapidly as the temperature increases to 90 K and 180 K, respectively, as shown in Fig. 3(a). It implies that the nonradiative recombination dominates, which leads to the quench of peaks B and C quickly as the temperature increases. Furthermore, for peak B, the high temperature quenching is explained by the release of holes from the acceptor. In fact, peak B appears at 90 K, while peak C appears up to 200 K. It is related to the neutral Ga_{As} center which must trap two photoexcited holes. Consequently, compared with Ga_{As}^{2-}, the luminescence peak of Ga_{As} occurs at lower temperatures. Additionally, peak C is the dominant emission peak up to 150 K. The luminescence behavior has been explained by an increased fraction of the singly ionized acceptor level.[19,27] The ionized acceptor concentration is much higher, which indicates that the growth quality of the sample M2 is not as good as that of sample M1.

To further determine the defect recombination mechanism, the PL spectra of sample M2 were measured at variable excitation power, as shown in Fig. 3(b). It can be observed that compared to the Ga_{As}^{2-} emission peak, the intensity of band-to-band emission becomes strengthened as the PL excitation power increases. It can be attributed to the saturation of carrier filling with high excitation density at the Ga_{As}^{2-} acceptor level. Moreover, it is worth pointing out that peaks B and C blueshift by 3.8 nm and 3.5 nm, respectively, with increases of the PL FWHMs, as the PL excitation power increases, which is caused by the band filling effect.[28] At higher excitation power, the photoexcited electrons fill the upper level of the conduction band. As the excitation power decreases, the electrons fill the bottom of the conduction band. As a consequence, as the excitation power increases, the peak shifts to higher energy, which leads to the blueshift and the increase of the PL FWHM, as shown in Fig. 4. Figure 5 shows the optical transition models of sample M2.

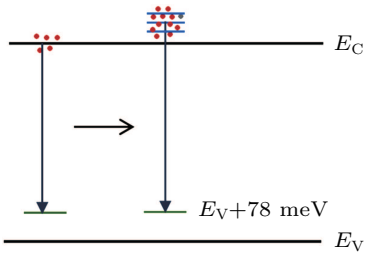


Fig. 4. Schematic energy diagram showing energy filling model.

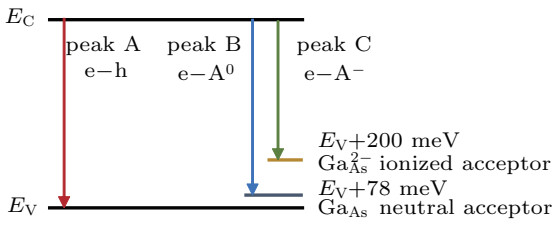


Fig. 5. Suggested energy band diagram for sample M2.

Figure 6 shows the photoluminescence spectra of sample M3. The peaks corresponding to the band-to-band emission are absent in Fig. 6(a), because the band-to-band transition is screened by a large concentration of the Ga_{As} deep acceptor at 77 K, which implies that the growth quality of sample M3 is poor. It can be seen that peak D is asymmetry at 77 K and there is another peak in the direction of higher energy at about 816 nm (1.52 eV), as shown in Fig. 6(a). This peak is most likely associated with the recombination of degenerate electron gas with the holes in the valence band of the heavily Si-doped GaAs.[24,29,30] With the increase of temperature, both peaks appear simultaneously and show a competitive trend. When the temperature is up to 120 K, the band-to-band transition becomes dominated and the peak of 78 meV Ga_{As} deep acceptor disappears. The dominated luminescence peak D at about 1.476 eV is due to a recombination involving the neutral state of the 78 meV Ga_{As} deep acceptor defect, which is observed in the heavily Si doped GaAs crystal as shown in Fig. 6(a). In this case, it can be observed that the energy of the Ga_{As} emission peak is higher than 1.44–1.45 eV reported in Refs. [12,19,26]. The authors of Refs. [8,24,29] attributed

the 1.45–1.47 eV emission peak to the recombination of electrons in the degenerate electron gas with holes bound to the Ga_{As} deep acceptor. This explanation should be valid for our heavily Si-doped samples.

The peak E observed at energy near 1.372 eV is attributed to the V_{As}–Si_{As} transition, which involves the deep-donor–shallow-acceptor complex transition[31–33] in Fig. 6(a). In this case, the donor is a V_{As}, whereas the acceptor is a Si atom on an As site (Si_{As}). A phonon replica of the 1.372 eV emission peak is observed at 1.307 eV labeled E^{1LO} in Fig. 6(a). The relationship between the intensity of the no-phonon 1.372 eV emission band, I^0_{PL}, and that of the n-th phonon replica, I^n_{PL}, is given by the Poisson distribution[34]

$$I^n_{PL} = I^0_{PL}\frac{\overline{N}^n}{n!}, \quad (n = 0, 1, 2, \ldots), \tag{2}$$

where $\overline{N}^n$ is the average number of LO phonons emitted together with one photon. Equation (2) reflects the coupling strength between the electron transition and the LO phonons. We find $N^n \approx 0.023$ for the acceptor, which agrees with $N^n \approx 0.02$–0.06 reported for shallow acceptors.[12] The weak coupling between the electron transition and LO phonons indicates that the 1.46 eV emission peak is associated with a shallow acceptor.

The emission peak F at 1.289 eV has an FWHM as large as 87 nm, as see in Fig. 6(a). This emission peak is related to the internal transition of V_{As}–Ga_{As} complex. The V_{As} is a donor with energy level at 145 meV below the conduction band.[3,10,35] Since V_{As} is a deep donor and Ga_{As} is a deep acceptor, they are bound together by the Coulombic force to form a localized donor–acceptor pair, which acts as a stationary molecule. The characteristic of the localized deep centers is the strong coupling between the electronic state and the lattice. For a strong enough electron–phonon interaction, the vibrational contribution results in a broad Gaussian line shape of the V_{As}–Ga_{As} emission peak, as see in Fig. 6(a).

In Fig. 6(b), it can be observed that the peak F blue shifts as the temperature increases from 77 K to 100 K. With the increase of the temperature, the carriers obtain energy and the donor–acceptor transition (localized state) becomes the free exciton transition. As a consequence, the band gap increases and the PL peaks show a blue shift. As the temperature increases, the luminescence intensity of peak D decreases more quickly compared with that of peak E. The peak position and the temperature-dependent behavior of peak D suggest that the carriers shift from high-energy state to low-energy state as the temperature increases, which results in the emission intensity of peak E higher than that of peak D. Because the carriers in the higher energy state are more easily excited, the intensity of peak D decreases more quickly than that of peak E. As the temperature further increases to 250 K, the band-to-band transition is dominant while peak E quenches. It can be observed that the integrated intensities for 78 meV Ga_{As} deep acceptor defect and V_{As}–Si_{As} complex (including the first phonon replica) quench at higher temperature. As the temperature increases, the escape of carriers is due to the intense thermal motion, which causes quenching of these peaks.

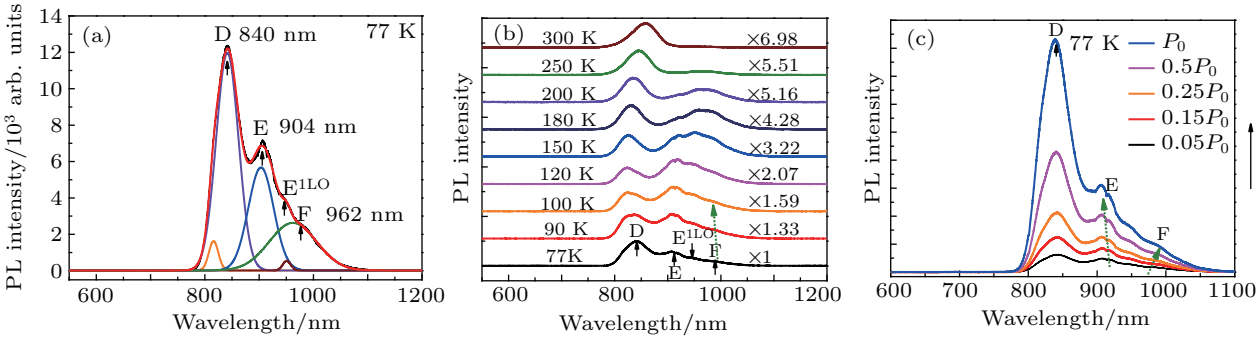


Fig. 6. PL spectra of sample M3, the heavily Si-doped GaAs crystal. (a) Gaussian fitting PL spectra of sample M3 at 77 K. (b) The normalized PL spectra taken at various temperatures. (c) 77 K PL spectra taken at various excitation power. The direction of the arrow represents an increase in excitation power.

As the excitation power increases, as shown in Fig. 6(c), peaks D and E blueshift by 3.8 nm and 6.5 nm, respectively. The former can be attributed to the band filling model as mentioned above, while the latter can be explained by the following formula:[36]

$$E_s = E_g - (E_A + E_D) + \frac{e^2}{4\pi\varepsilon r}, \tag{3}$$

where E_s is the donor–acceptor (DA) pair recombination energy, E_g is the bandgap energy, E_A is the acceptor ionization energy, E_D is the donor ionization energy, r is the distance between the DA pair, e is the electronic charge, and ε is the dielectric constant. With the excitation power increase, the radiative recombination between the DA pairs separated by large distances is saturated. Therefore, at higher excitation power density, E_s increases as the involved value of r becomes smaller, which leads to the blueshift, as can be seen in Fig. 7.

The different behavior of peak F due to the V_{As}–Ga_{As} complex (deep-donor–deep-acceptor) transition. As the excitation power increases, peak F redshifts, as can be seen in Fig. 6(c). The phenomenon is due to the heating effect of the

laser on the sample lattice. It can be concluded that with an increase of power, the thermal expansion effect of the crystal lattice and the partial energy of the carrier transmitted to the crystal lattice in the form of phonons lead to the redshift of the lower-energy side. Since very few carriers participate in the V_{As}–Ga_{As} transition, the blueshift effect at variable power is basically offset by the red shift caused by the thermal effect. Therefore, as the power increases, peak F shows a redshift phenomenon. Figure 8 shows the optical transition models of sample M3.

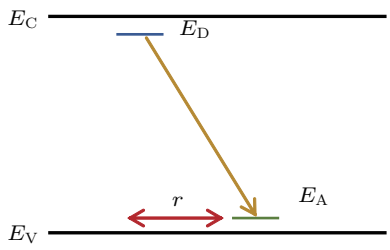


Fig. 7. Transition of donor and acceptor.

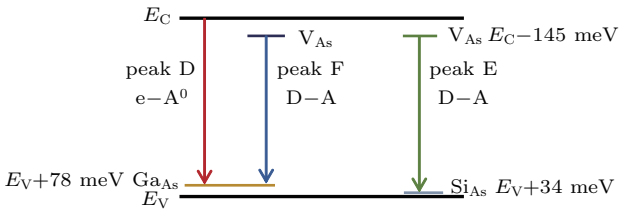


Fig. 8. Suggested energy band diagram for sample M3.

From this paper, it can be seen that the incorporation of impurity elements into GaAs crystals introduces defect levels, but has no significant effect on the crystal quality. The crystal quality of the GaAs substrate is mainly determined by its native defect states.

4. Conclusions

In summary, we have investigated the defect-related PL spectra of N-type GaAs substrates. We observed the Ga_{As} antisite defect in both samples doped with Si, which is the double-acceptor defect in GaAs. However, there is a difference in PL between lightly doped and heavily doped samples. By systematically analyzing the temperature-dependent and variable power PL spectra, optical transition models were established. We analyzed the defect states and their luminescence mechanisms. It can be concluded that the crystal quality of the GaAs substrate is mainly determined by its native defect states and the growth quality of sample M1 is good.

References

[1] Li M F, Ni H Q, Ding Y, David B, Liang K, Ana C M and Niu Z C 2014 *Chin. Phys. B* **23** 027803
[2] Xu J B, Zhang H Y, Fu X J, Guo T Y and Huang J 2010 *Chin. Phys. B* **19** 037302
[3] Ali Y P, Narsale A M and Arora B M 2006 *Nucl. Instr. Meth. Phys. Res. B* **247** 238
[4] Baeumler M, Börner F, Kretzer U, Scheffer-Czygan M, Bünger T and Wagner J 2008 *J. Mater. Sci: Mater Electron.* **19** 165
[5] Choi H Y, Cho M Y, Yim K G, Kim M S, Lee D Y, Kim J S, Kim G S and Leem J Y 2012 *Microelectron. Eng.* **89** 6
[6] Lavrukhin D V, Yachmenev A E, Bugaev A S, Galiev G B, Klimov E A, Khabibullin R A, Ponomarev D S and Maltsev P P 2015 *Semiconductors* **49** 911
[7] Galiev G B, Klimov E A, Klochkov A N, Pushkarev S S and Maltsev P P 2018 *Semiconductors* **52** 376
[8] Ky N H and Reinhart F K 1998 *J. Appl. Phys.* **83** 718
[9] Xu H and Lindefelt U 1990 *Phys. Rev. B* **41** 5979
[10] Wager J F 1991 *J. Appl. Phys.* **69** 3022
[11] Yu P W 1984 *Phys. Rev. B* **29** 2283
[12] Y P W and Reynolds D C 1982 *J. Appl. Phys.* **53** 1263
[13] Elliott K R 1983 *Appl. Phys. Lett.* **42** 274
[14] Chatterjee P K, Vaidyanathan K V, Durschlag M S and Streetman B G 1975 *Solid State Commun.* **17** 1421
[15] Hwang C J 1969 *Phys. Rev.* **180** 827
[16] Birey H and Sites J 1980 *J. Appl. Phys.* **51** 619
[17] Bogardus E H and Bebb H B 1968 *Phys. Rev.* **176** 993
[18] Williams E W 1968 *Phys. Rev.* **168** 922
[19] Bugajski M, Ko K H, Lagowski J and Gatos H C 1989 *J. Appl. Phys.* **65** 596
[20] Hetzler S R, McGill T C and Hunter A T 1984 *Appl. Phys. Lett.* **44** 793
[21] Shanabrook B V, Moore W J and Bishop S G 1986 *J. Appl. Phys.* **59** 2535
[22] Suezawa M and Sumino K 1994 *J. Appl. Phys.* **76** 932
[23] Yu P W, Mitchel W C, Mier M G, Li S S and Wang W L 1982 *Appl. Phys. Lett.* **41** 532
[24] Piazza F, Pavest L, Henini M and Johnston D 1992 *Semicond. Sci. Technol.* **7** 1504
[25] Moore W J, Hawkins R L and Shanabrook B V 1987 *Physica B+C* **146** 65
[26] Mihara M, Mannoh M, Shinozaki K, Naritsuka S and Ishii M 1986 *Jpn. J. Appl. Phys.* **25** L611
[27] Kressel H, Dunse J U, Nelson H and Hawrylo F Z 1968 *J. Appl. Phys.* **39** 2006
[28] Kulakovskii V D, Lach E and Forchel A 1989 *Phys. Rev. B* **40** 8087
[29] Pavesi L, Henini M and Johnston D 1995 *Appl. Phys. Lett.* **66** 2846
[30] Borghs G, Bhattacharyya K, Deneffe K, Van Mieghem P and Mertens R 1989 *J. Appl. Phys.* **66** 4381
[31] Mokerov V G, Fedorov Yu V, Guk A V, Galiev G B, Strakhov V A and Yaremenko N G 1998 *Semiconductors* **32** 950
[32] Seong H and Lewis L J 1995 *Phys. Rev. B* **52** 5675
[33] Islam A Z M T, Jung D W, Noh J P and Otsuka N 2009 *J. Appl. Phys.* **105** 093507
[34] Hopfield J J 1959 *J. Phys. Chem. Solids* **10** 110
[35] Ha Y K, Lee C, Kim J E and Park H Y 2000 *J. Korean Phys. Soc.* **36** 42
[36] Thomas D G, Gershenzon M and Trumbore F A 1964 *Phys. Rev.* **133** A269